MGPB

Time effect of pile-soil interaction and its elastic-viscoplastic constitutive model

The Mining-Geology-Petroleum Engineering Bulletin
UDC: 551:24
DOI: 10.17794/rgn.2019.1.1

Original scientific paper

Hong-quan Li[1,2]; Sheng-yang Feng[3*]; Li-min Wei[1]; Zhi Chen[3]

[1]*School of Civil Engineering, Central South University, Changsha, China*
[2]*Hunan Provincial Communications Planning, Survey & Design Insitute Co., Ltd., Changsha, China*
[3]*School of Environment and Safety Engineering, University of South China, Hengyang, China*

Abstract

Pile-soil interaction is considered to be one of the most important problems in the study of the mechanical behaviour of pile foundation. In this paper, the lateral friction resistance and pile-soil relative displacement of bridge piles in deep soft soils are monitored for an extended period by using concrete strain gauges that are embedded in the test pile. Field test results show that both the pile lateral frictional resistance and pile-soil relative displacement increase along with time, while the pile-soil interaction demonstrates a time effect. Therefore, an elastic-viscoplastic constitutive model must be established to better simulate the time-dependent mechanical behaviour of the pile-soil contact. Based on the Goodman model, we developed an elastic-viscoplastic interface constitutive model of the pile-soil interface into the FRIC subroutine through ABAQUS software, which is one of the most commonly used finite element analysis softwares in the world, to simulate a well-recorded pile test in deep soft soils. The calculated pile lateral frictional resistance and pile-soil relative displacement are close to the measured values, and the ability of the interface model to describe the changes in the shear stress-strain of the pile-soil interface along with time is validated.

Keywords:

pile-soil interaction, time effect, elastic-viscoplastic constitutive model, lateral friction resistance, pile-soil relative displacement

1. Introduction

Pile-soil interaction is one of the most difficult problems in the field of geotechnical engineering. Given the great difference between the properties of the pile material and the surrounding soil, the characteristics of the pile-soil interaction is highly nonlinear and very complex. Many researchers (**Zou et al., 2006; Mabsout et al., 2010; Chen et al., 2011; Liu et al., 2012; Zhao et al., 2013; Sheng-yang et al., 2014; Jun, 2015; Yang et al., 2015; Abu-Farsakh et al., 2017; Hussein et al., 2017**) have applied numerical simulation for analyzing this pile-soil interaction problem.

The numerical simulation of the mechanical behavior of the pile-soil interaction focuses on two aspects, namely, the interface element and the interface constitutive model or the relationship between the shearing stress and shear deformation of the pile-soil interface. The interface element can be divided into non-thickness and thin-thickness interface elements, where the former mainly includes the Goodman element (**Goodman et al., 1968**) and the improved non-thickness spring element (**Ghaboussi et al., 1973**) while the latter mainly includes the thin-thickness element proposed by **Desai et al. (1984)** and **Yin et al. (1994)**. The Goodman element not only simulates the shear stress-strain of the pile-soil interface but also considers the discontinuity between the pile and soil interface. Given that its parameters have clear physical meaning and concept, the Goodman element has been widely used for numerically simulating the pile-soil interaction problem.

The nonlinear elastic model based on the hyperbolic model of Clough and Duncan (**Clough et al., 1971**) has been widely used to illustrate the constitutive relation of the interface. **Boulon et al. (1990)** proposed the elastic-plastic model, which constructs a constitutive relation similar to that constructed by the hyperbolic model. At present, the constitutive relation of the interface is mainly constructed by using the two aforementioned models, but **An et al. (2001)**, **Guo (2000a; 2000b)**, and **Li et al. (2015)** argue that the relationship between the stress and relative displacement of the interface also needs to consider the time effect. Therefore, it is very necessary to establish a pile-soil interface constitutive model to better simulate the time-dependent mechanical behaviour of the pile-soil contact.

In this paper, we carried out field tests to monitor the lateral friction resistance and pile-soil relative displacement of bridge piles in deep soft soils for an extended period. Through the field tests, we found out the rule of

Corresponding author: Sheng-yang Feng
14100044@usc.edu.cn

the pile-soil interaction variation with time. Then, based on the time-dependent rule of the pile-soil interaction, a pile-soil interface elastic-viscoplastic constitutive model is proposed and developed into the FRIC subroutine in ABAQUS. The proposed model can be used to better simulate the pile foundation engineering problems by the finite element method.

2. Field test

To understand the lateral friction and pile-soil relative displacement variations in deep soft soils, a large number of concrete strain gauges have been embedded in the center pile of the No. 667 bridge pier of Ningbo Bridge in the Hangzhou–Ningbo high-speed railway. The bridge pier has a pile length and diameter of 63.5 m and 1 m, respectively, while the soft soil layer has a thickness of 35.3 m. The bearing layer is a hard silty clay with a bearing capacity of 180 kPa. The field test is carried out according to the following steps:

(1) Twenty test sections are selected for the test pile, with each section symmetrically equipped with two strain gauges, thereby amounting to a total of 40 strain gauges. Strain gauges are tied to the pile's steel bar according to the arrangement of the strain gauges in the test pile (see **Figure 1**), shown in **Figure 2**.

(2) Weld the steel cage of the test pile in the order of the arrangement of the strain gauges in the test pile, then hoist the steel cage into the pile hole, and finally pour the concrete. The test pile construction can be shown in **Figure 3**. After the concrete is solidified, the strain of the pile can be measured.

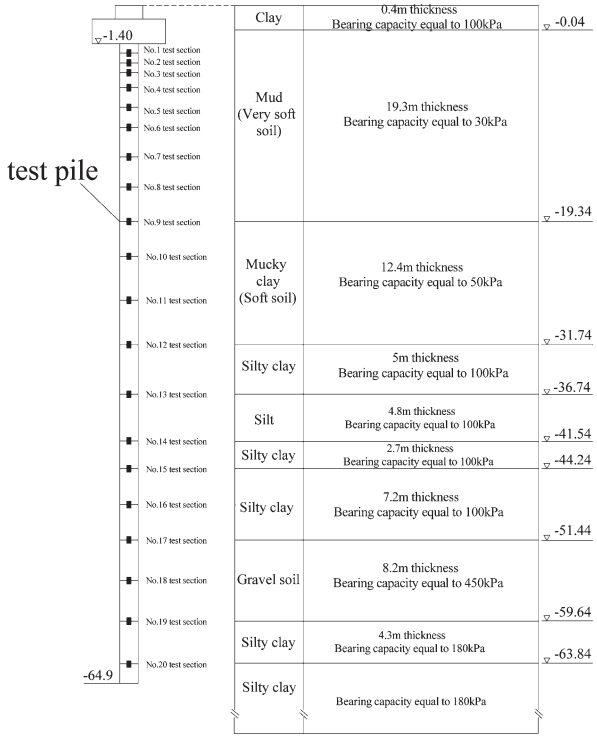

Figure 1: Arrangement of the strain gauges in the test pile (unit: meter)

(3) Before erecting the bridge beam and completing the construction of the pier, the load on the pile foundation can be regarded as unchanged. During this period, the strain of the test pile is monitored for 317 days.

(4) The initial value of the concrete strain gauge is measured after the final solidification of the pile concrete. After loading the pile foundation, the measured value of the strain gauge is calculated. Both the initial and measured values are affected by temperature, which needs to be modified. The difference between the measured and initial values is regarded as the strain of the pile at some test sections, and the pile axial force at the test section can be calculated by the elastic modulus of the pile. The pile axial force at test section i can be calculated as

$$N_{\mathrm{i}} = E\,\bar{\varepsilon}_{\mathrm{i}}\,A\,, \tag{1}$$

where E is the elastic modulus of the pile, and $\bar{\varepsilon}_{\mathrm{i}}$ is the average measured strain of section i.

The frictional resistance of the pile, f, can be expressed as

$$f_i = \frac{N_{\mathrm{i}} - N_{\mathrm{i+1}}}{Ul_i}\,, \tag{2}$$

where U is the circumference of the pile section, and l_{i} is the length between sections i and i+1.

According to reference (**Zhang et al., 2004**), the pile-soil relative displacement, ω_{i}, in section i can be written as

$$w_{\mathrm{i}} = w_0 - \sum_{j=1}^{i} \frac{l_{\mathrm{i}}}{2}(\bar{\varepsilon}_{\mathrm{j}} + \bar{\varepsilon}_{\mathrm{j+1}})\,, \tag{3}$$

where w_0 is the displacement of the pile top.

The pile lateral friction resistance can be calculated by **Equations 1** and **2**, and the pile lateral friction resistance profiles at different times can be seen in **Figure 4**. **Figure 5** shows the variations in pile lateral friction resistance with time at different depths. The pile lateral friction resistance increases as the pile depth increases from 0 m to 30.36 m, where the pile is located in soft soil layers. Meanwhile, from 30.36 m to the pile bottom, the pile lateral friction decreases along with an increasing pile depth. The pile lateral friction resistance of the upper part has a higher increase rate than that of the lower part, and the pile lateral friction resistance shows a time dependence.

The pile-soil relative displacement can be calculated by **Equation 3**, and the pile-soil relative displacement profiles at different times are shown in **Figure 6**. **Figure 7** presents the variations in pile-soil relative displacement with time at different depths. The pile-soil relative displacement decreases along with an increasing pile depth, and the increase rate of the pile-soil relative displacement from 0 days to 89 days is much larger than that recorded at later periods. The pile-soil relative displacement also produces a time effect.

The above analysis shows that both the pile lateral friction resistance and pile-soil relative displacement

Figure 2: Installation of strain gauges on the test pile

Figure 3: Test pile construction

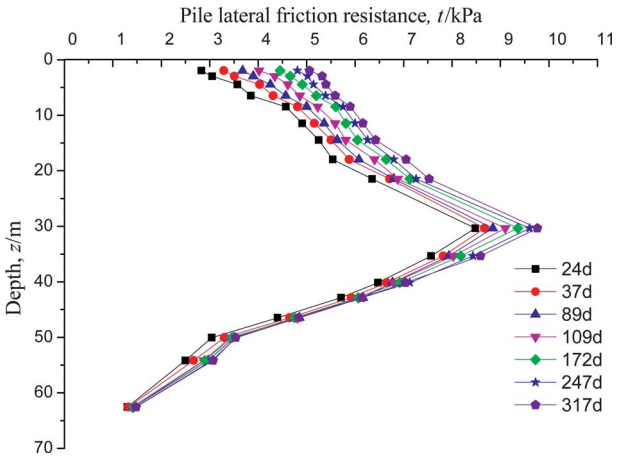

Figure 4: Pile lateral friction resistance profiles at different times

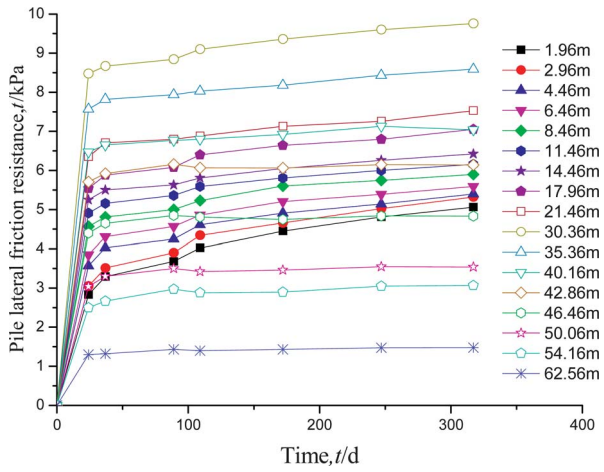

Figure 5: Pile lateral friction resistance changing with time at different depth

have a time effect. However, given that the pile-soil interface models currently do not take into account the time effect, the pile-soil interface model cannot reflect the true pile-soil interface relationship in the strict sense. Therefore, the constitutive relationship of the pile-soil interface must consider the time effect. To better simulate the pile-soil interaction problem in soft soils, a pile-soil interface model that considers the time effect must be developed.

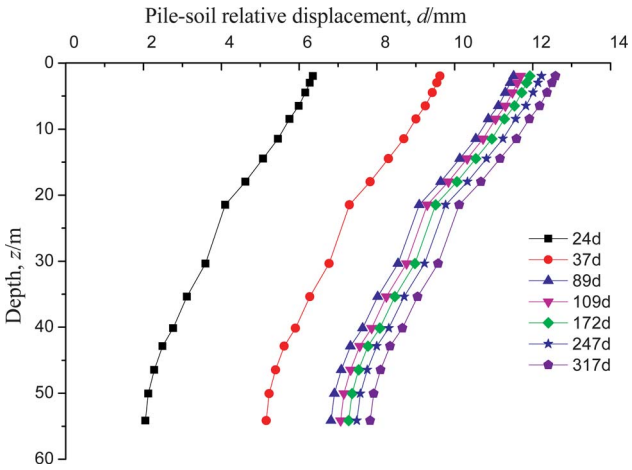

Figure 6: Pile-soil relative displacement profiles at different times

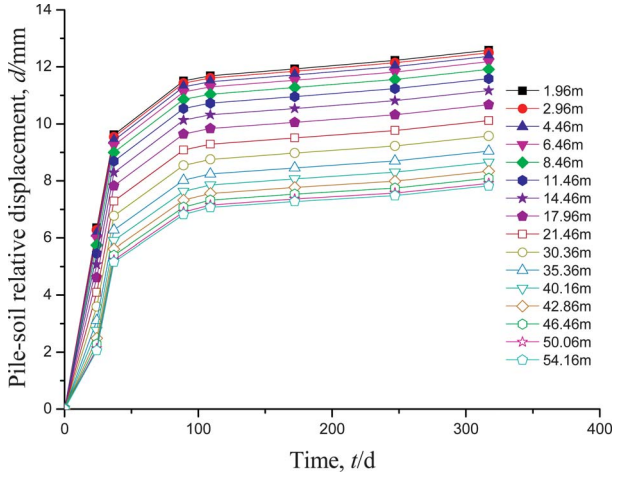

Figure 7: Pile-soil relative displacement changing with time at different depth

3. Elastic-viscoplastic interface constitutive model of the pile-soil interface

The elastic interface constitutive relation of the pile-soil interface can be expressed by (**Goodman et al., 1968**)

$$\{\Delta\tau\} = \begin{bmatrix} k_{s1} & 0 \\ 0 & k_{s2} \end{bmatrix} \{\Delta\gamma^{e}\}, \tag{4}$$

where $\{\Delta\tau\} = [\Delta\tau_1\ \Delta\tau_1]^T$, in which $\Delta\tau_1$ and $\Delta\tau_2$ are the shear stress increments in two tangential directions of the interface; $\{\Delta\gamma^e\} = [\Delta\gamma_1^e\ \Delta\gamma_2^e]^T$, in which $\Delta\gamma_1^e$ and $\Delta\gamma_2^e$ are the elastic shear strain increments in two tangential directions of the interface; and k_{s1} and k_{s2} are the tangential stiffness coefficients in two tangential directions of the interface. Based on the direct shear test results, **Clough and Duncan (1971)** argued that the relationship between the shear stress, τ, and relative displacement, ω, in the tangential direction of the interface is hyperbolic and can be written as

$$\tau = \frac{\omega}{a + b\omega}, \tag{5}$$

$$a = \frac{1}{Kr_w\left(\sigma_n / P_a\right)^n}, \text{ and} \tag{6}$$

$$b = \frac{R_f}{\sigma_n \tan\delta}, \tag{7}$$

where K, n, and R_f are nonlinear indexes that can be determined via the direct shear test, δ is the interface friction angle of the interface, r_w is the water unit weight, P_a is the atmospheric pressure, and σ_n is the normal stress.

By taking the above hyperbolic model as the interface constitutive relation of the pile-soil interface in the elastic stage, the tangential stiffness coefficient can be expressed as

$$\begin{cases} k_{s1} = \dfrac{d\tau}{d\omega} = \left(1 - R_f \dfrac{\tau_1}{\sigma_n \tan\delta}\right)^2 Kr_w \left(\dfrac{\sigma_n}{P_a}\right)^n \\ k_{s2} = \left(1 - R_f \dfrac{\tau_2}{\sigma_n \tan\delta}\right)^2 Kr_w \left(\dfrac{\sigma_n}{P_a}\right)^n \end{cases}. \tag{8}$$

The tensor of the viscoplastic shear strain increment of the interface can be written as

$$\Delta\gamma_{ij}^{vp} = \frac{1}{\eta}\left\langle\Phi(F/F_0)\right\rangle \frac{\partial Q}{\partial\sigma_{ij}}\Delta t, \tag{9}$$

where

$$\left\langle\Phi(F/F_0)\right\rangle = \begin{cases} \Phi(F/F_0), F/F_0 > 0 \\ 0, F/F_0 \le 0 \end{cases}, \tag{10}$$

where η is the viscosity coefficient that can be fitted by the datum from the rheological shear test of the interface, F is the yield function, F_0 is the reference value of the yield function, Φ is a function that defines the viscoplastic strain rate $\Phi(F) = [(F - F_0)/F_0]^N$ in this paper, where N=1 for geotechnical material) (**Swoboda et al., 1987**), Q is the plastic potential function, σ_{ij} is the stress tensor of the interface, and Δt is the time increment.

This paper applies the Drucker–Prager yield criterion, which yield function is expressed as

$$F = \sqrt{J_2} + \alpha I_1 - k. \tag{11}$$

The reference value F_0 corresponding to the Drucker–Prager yield function can be written as (**Swoboda et al., 1987**)

$$F_0 = \frac{6c\cos\phi}{\sqrt{3}(\sqrt{3} - \sin\phi)}, \tag{12}$$

where α and k are parameters of the Drucker–Prager yield criterion, J_2 is the second principal stresses invariant, and I_1 is the major principal stress invariant. If the Drucker–Prager cone and the Mohr–Coulomb hexagonal cone are externally connected, the relationship between the parameters of the Drucker–Prager yield crite-

rion (i.e., α and k) and those of the Mohr–Coulomb yield criterion (i.e., c (cohesion) and φ (internal friction angle)) can be written as

$$\left.\begin{aligned}\alpha &= \frac{2\sin\phi}{\sqrt{3}(3-\sin\phi)}\\ k &= \frac{6c\cos\phi}{\sqrt{3}(3-\sin\phi)}\end{aligned}\right\}. \tag{13}$$

If the associated flow rules for the Drucker–Prager yield criterion are used (i.e., Q=F), then

$$\frac{\partial Q}{\partial \sigma_{ij}} = \frac{\partial F}{\partial \sigma_{ij}} = \alpha\delta_{ij} + \frac{S_{ij}}{2\sqrt{J_2}}(i,j=1,2,3), \tag{14}$$

where δ_{ij} is the Kronecker delta, and S_{ij} is the deviatoric stress tensor.

Three stresses, including normal stress, σ_n, and two tangential shear stresses, τ_1, τ_2, are present in the interface element. Therefore,

$$\begin{cases} I_1 = \sigma_{xx} + \sigma_{yy} + \sigma_{zz} = \sigma_n \\ J_2 = \frac{1}{2}S_{ij}S_{ij} = \frac{1}{3}\sigma_n^2 + \tau_1^2 + \tau_2^2 \end{cases}. \tag{15}$$

To be consistent with **Equation 4**, $\Delta\gamma_{ij}^{vp}$ can be converted into its vector form as $\left\{\Delta\gamma^{vp}\right\} = \left[\Delta\gamma_1^{vp} \quad \Delta\gamma_2^{vp}\right]^T$.

Assuming that the strain increment of the interface under each load step, $\{\Delta\gamma\}$, can be divided into the elastic strain increment, $\{\Delta\gamma^e\}$ and the viscoplastic strain increment, $\{\Delta\gamma^{vp}\}$, the constitutive relation of the pile-soil interface under the viscoplastic condition can be expressed as

$$\{\Delta\tau\} = \begin{bmatrix} k_{s1} & 0 \\ 0 & k_{s2} \end{bmatrix}\left(\{\Delta\gamma\} - \left\{\Delta\gamma^{vp}\right\}\right). \tag{16}$$

4. Secondary development in ABAQUS

In the FRIC user subroutine of ABAQUS, only the frictional interface characteristics on the interface must be considered while the local coordinate system of the interface must not be taken into account. The main program of ABAQUS decides whether the interface is detached or not. Based on the established elasto-viscoplastic constitutive model of the pile-soil interface, the interface constitutive model in ABAQUS is developed by the FRIC user subroutine. The flow chart of the FRIC user subroutine of the elasto-viscoplastic constitutive model of the pile-soil interface is shown in **Figure 8**. The process is summarized as follows:

(1) At the nth load step, the main program in ABAQUS calls the FRIC user subroutine and transfers the datum to the FRIC user subroutine, including the interface pressure (normal stress ${}^n\sigma_n$), interface shear stress (two tangential shear stresses, ${}^n\tau_1$ and ${}^n\tau_2$), shear stiffness (${}^nk_{s1}$ and ${}^nk_{s2}$), interface state (whether the interface is detached or not), and time increment (Δt).

(2) **Equation 10** determines whether the interface is in an elastic state or in a visco-plastic state.

In the elastic state, the interface shear stress increments at the nth load step, $\Delta^n\tau_1$, $\Delta^n\tau_2$, are calculated by **Equation 4**, those at the (n+1)th load step can be updated by ${}^{n+1}\tau_1 = {}^n\tau_1 + \Delta^n\tau_1$, ${}^{n+1}\tau_2 = {}^n\tau_2 + \Delta^n\tau_2$, and the shear stiffness at the (n+1)th load step, ${}^{n+1}k_{s1}$, ${}^{n+1}k_{s2}$, can be updated by **Equation 8**.

In the visco-plastic state, the interface shear stress increments at the nth step, $\Delta^n\tau_1$, $\Delta^n\tau_2$, are calculated by **Equation 16**, those at the (n+1)th load step can be updated by ${}^{n+1}\tau_1 = {}^n\tau_1 + \Delta^n\tau_1$, ${}^{n+1}\tau_2 = {}^n\tau_2 + \Delta^n\tau_2$, and the shear stiffness of the (n+1)th load step, ${}^{n+1}k_{s1}$, ${}^{n+1}k_{s2}$, also can be updated by **Equation 8**.

The above datum at the (n+1)th load step are sent back to the main program in ABAQUS.

(3) The main program in ABAQUS performs the iterative computation at the (n+1)th load step with a default maximum iteration number of 9 and a minimum tolerance of 0.005. When the error of the iterative computation is less than the minimum tolerance, the iterative computation is convergent and the program automatically performs the iteration of the next incremental step.

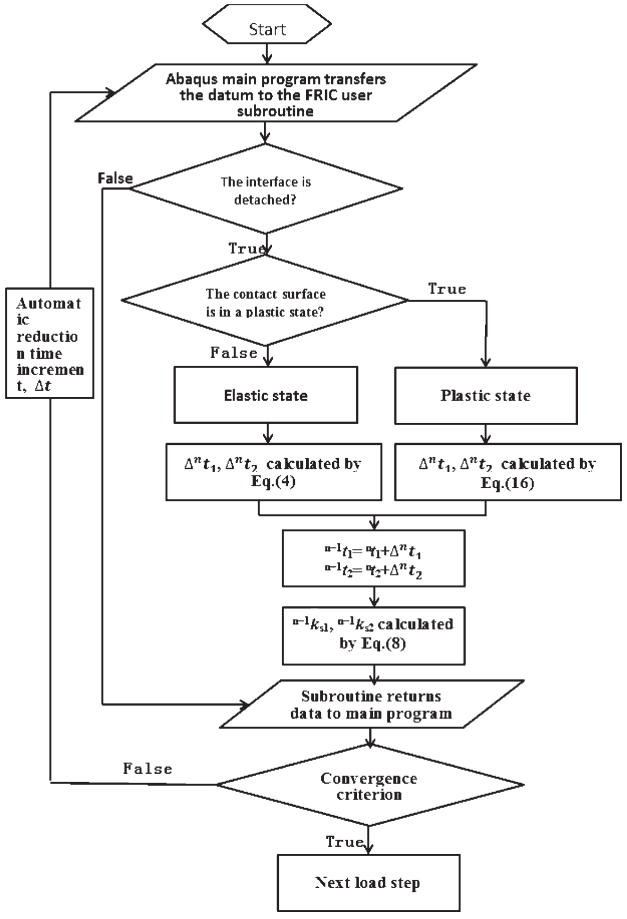

Figure 8: The flow chart of the FRIC user subroutine

If the iterative computation is not convergent, then the main program in ABAQUS automatically reduces the time increment and performs the iterative calculation again until the result converges.

Based on the above steps, the FRIC user subroutine is developed by using Intel Visual Fortran 11.1.

5. Verification

The pile foundation of the No. 667 bridge pier of Ningbo Bridge in the Hangzhou–Ningbo high-speed railway is numerically simulated by using the established elastic-viscoplastic interface constitutive model of the pile-soil interface. The pile foundation comprises nine concrete cast-in-place piles with a 1 m diameter and a 64.5 m length. The horizontal, longitudinal, and vertical dimensions of the cap are 10.1, 7.4, and 2.5 m, respectively, as shown in **Figure 9**.

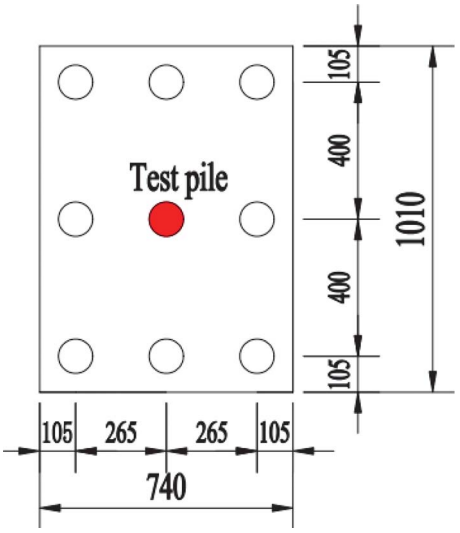

Figure 9: Design drawing of Pier 667# (Unit: cm)

The elastic constitutive model is used for the pile cap and piles. The elastic modulus, Poisson's ratio, and density are equal to 32.3 GPa, 0.17, and 2500 kg/m^3, respectively. The elastoplastic-consolidation coupled model is used for the soils, and the model parameters of each soil layer are given in **Table 1**.

Given that each pile is stratified according to the thickness of each soil layer, 10 pile-soil interfaces are established for each pile. A total of 90 pile-soil interfaces are established for the pile foundation. The FRIC user subroutine is used to simulate the pile-soil surfaces, and the parameters r_w = 10kN/m^3, P_a=101kPa, and α, k of each soil layer can be calculated by **Equation 13**. The interface friction angle of the pile-soil interface can be determinated by the friction interaction coefficient (Gradiki et al., 2017) or the following formula as

$$\delta = \tan^{-1}\left(\frac{\sin\phi\cos\phi}{1+\sin^2\phi}\right), \tag{17}$$

where K, n, R_f, and η can be obtained by fitting the curve between the pile lateral frictional resistance and the pile-soil relative displacement of each soil layer. The K, n, R_f, and η of each soil layer are listed in **Table 1**.

The ABAQUS software is used to establish the 3D finite element analysis model of the pile foundation, as shown in **Figure 10**. The transverse, longitudinal and vertical directions of the model are 101m, 75m, and 130.5 m. The total load on the pile foundation is 10856 kN, and the numerical simulation time is 317 days. The eight-node hexahedron element (C3D8 in ABAQUS) is used for the pile cap, piles and soils.

It is believed that the mesh size of the soil far away from the pile has little effect on the finite element analysis of the pile foundation, while the mesh size of the soil around the pile has a great influence. Therefore, soils around piles in the finite element analysis are divided into fine meshes, and those far away from piles are divided into coarse meshes. However, too fine mesh is

Table 1: Parameters of the elastoplastic-consolidation coupled model

Soil layer	H /m	γ /(kN/m^3)	E /MPa	μ	φ/°	c /kPa	k_v/×10^{-12} m.d^{-1}	e_0	δ/°	K	n	R_f	η/ MPa.d
(1) Clay	0.4	17.8	6.8	0.35	6.6	14.8	2.00	0.9	6.4	515	0.42	0.11	7.42
(2) Mud	19.3	16.9	3.0	0.42	2.6	5.6	0.06	1.2	2.6	296	0.29	0.27	6.23
(3) Mucky clay	12.4	17.4	3.7	0.40	4.0	10.2	0.14	1.1	4.0	408	0.28	0.28	6.40
(4) Silty clay	5.0	18.5	7.7	0.35	6.6	18.4	1.16	0.8	6.4	527	0.41	0.13	12.31
(5) Silt	4.8	19	21.5	0.30	25.0	7.4	69.44	0.7	18.0	771	0.40	0.08	27.00
(6) Silty clay	2.7	18.5	7.8	0.35	6.6	18.4	1.16	0.8	6.4	559	0.43	0.10	10.61
(7) Silty clay	7.2	18.5	8.3	0.35	6.5	18.7	1.16	0.8	6.3	623	0.45	0.10	11.99
(8) Gravel soil	8.2	19	30.0	0.23	35	0	20833	0.4	19.5	820	0.52	0.09	53.27
(9) Silty clay	4.3	19	14.5	0.28	15	39.9	1.00	0.8	13.2	787	0.45	0.10	17.65
(10) Silty clay	/	19	29.3	0.28	12.6	45	1.00	0.8	/	/	/	/	/

H – Soil layer thickness; γ – Water unit weight; E – Young's modulus; μ – Poisson's ratio; φ – internal friction angle; c – cohesion; k_v – Permeability coefficient; e_0 – Initial void ratio; δ – Interface friction angle of the interface; K, n, and R_f – Nonlinear indexes that can be determined by the direct shear test; and η – Viscosity coefficient.

computationally expensive, while too coarse mesh may yield in a slightly inaccurate result. Finding the appropriate mesh size is one of the key problems in finite element analysis of pile foundation. Therefore, the mesh size sensitivity analysis of the soil around the pile is carried out in this paper. We take the settlement of pile foundation as the judging basis of the mesh size sensitivity analysis. Table 2 lists settlement of the pile foundation calculated by numerical simulation with different mesh sizes. It indicates that the settlement of pile foundation decreases with a decrease in mesh size. When the mesh size is reduced to 0.3 m, the settlement of pile foundation is basically stable. When the mesh size is reduced to 0.1 m, the settlement decreases 0.1 cm compared with the mesh size 0.3 m, but the calculation time increases by 526%. Therefore, considering the accuracy of numerical simulation and the computation time, the optimal mesh size of the finite element analysis model in this paper is 0.3m.

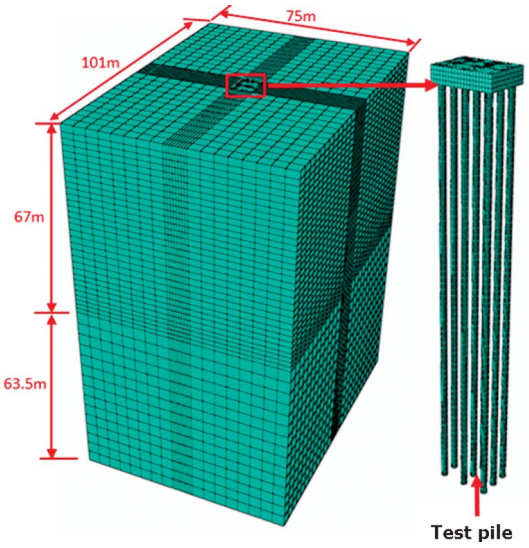

Figure 10: 3D FEM of No. 667 pier

Table 2: Settlement of pile foundation calculated by numerical simulation with different mesh sizes

Mesh size (m)	Element number	Computation Time (hour)	Settlement of pile foundation (cm)
1	57108	0.2	36.5
0.8	63553	0.9	35.2
0.6	71141	1.2	34.6
0.3	105522	6.8	30.3
0.1	255221	42.6	30.2

Figure 11 presents finite element simulation results of the pile-soil relative displacement and pile lateral friction resistance of the bridge pile foundation. The measured pile-soil relative displacements of the Nos. 1, 5, 11, and 17 test sections are compared with the numerical simulation results as shown in **Figure 12**. The numerical simulation results of the pile-soil relative displacement are close to the measured results, and the variation trend of the pile-soil relative displacement with time as captured in numerical simulation is consistent with the measured trend. The relative error between the simulated pile-soil relative displacement and the measured results is less than 15% in most cases, but only a few of them are relatively large in the initial stage of loading.

The measured pile lateral frictional resistances of the Nos. 1, 5, 11, and 17 test sections are compared with the results of numerical simulation as shown in **Figure 13**. The numerical simulation results for pile lateral frictional resistance are close to the measured results, and the variation trend of the pile lateral frictional resistance with time as captured in the numerical simulation is con-

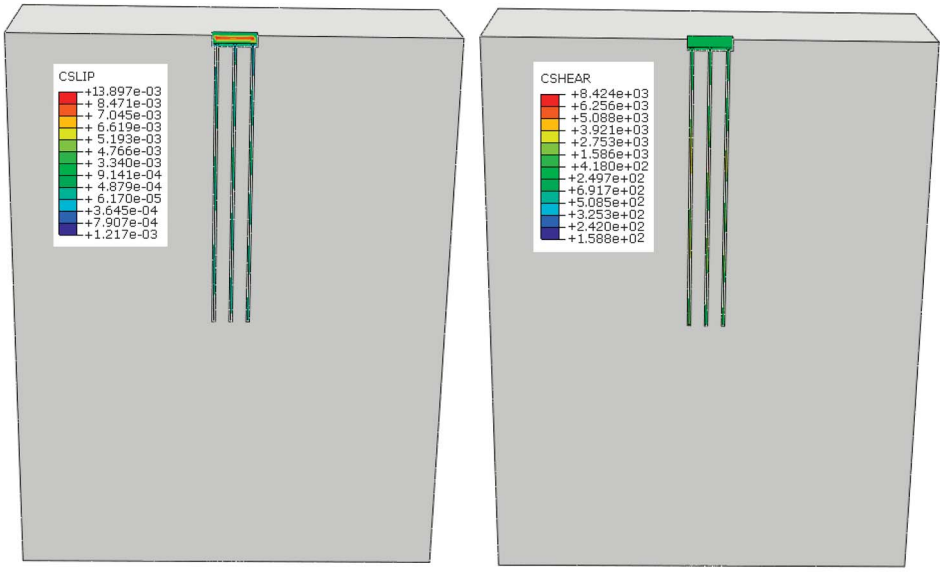

(a) Pile-soil relative displacement (b) Pile lateral friction resistance

Figure 11: Finite element numerical simulation results

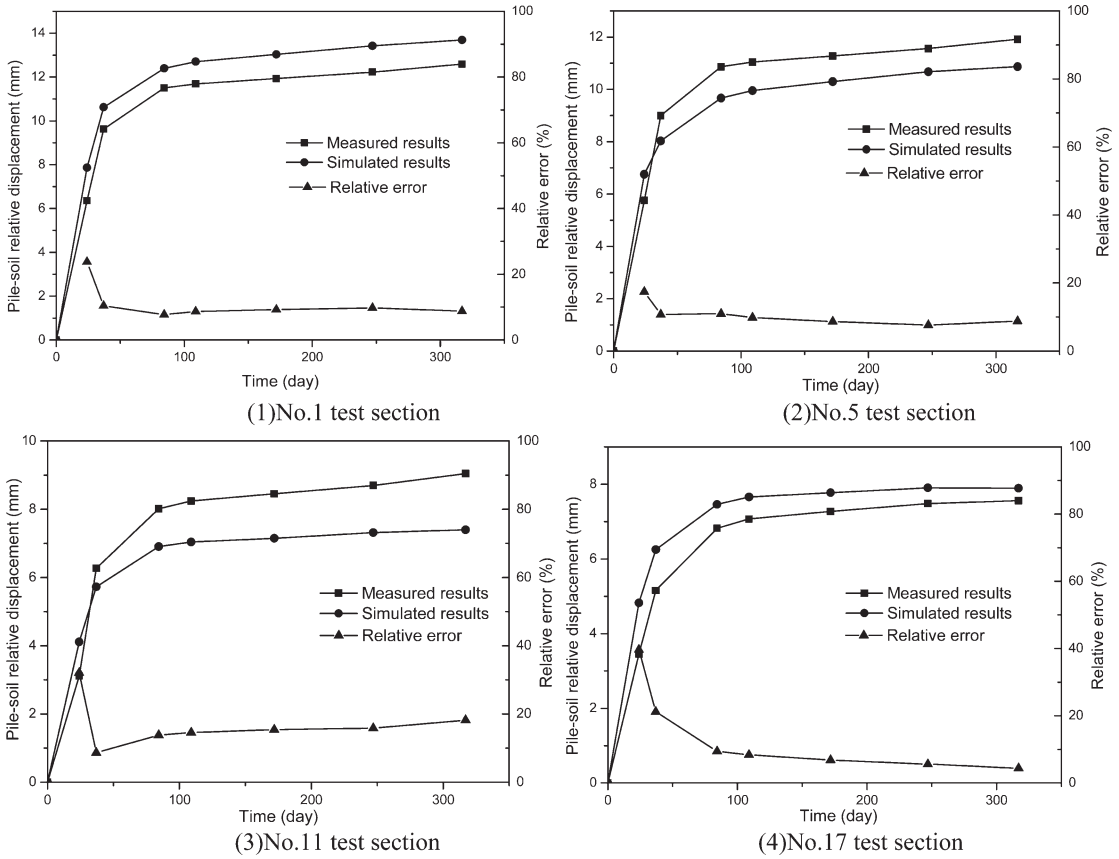

Figure 12: Comparison of the simulated pile-soil relative displacement and the measured results

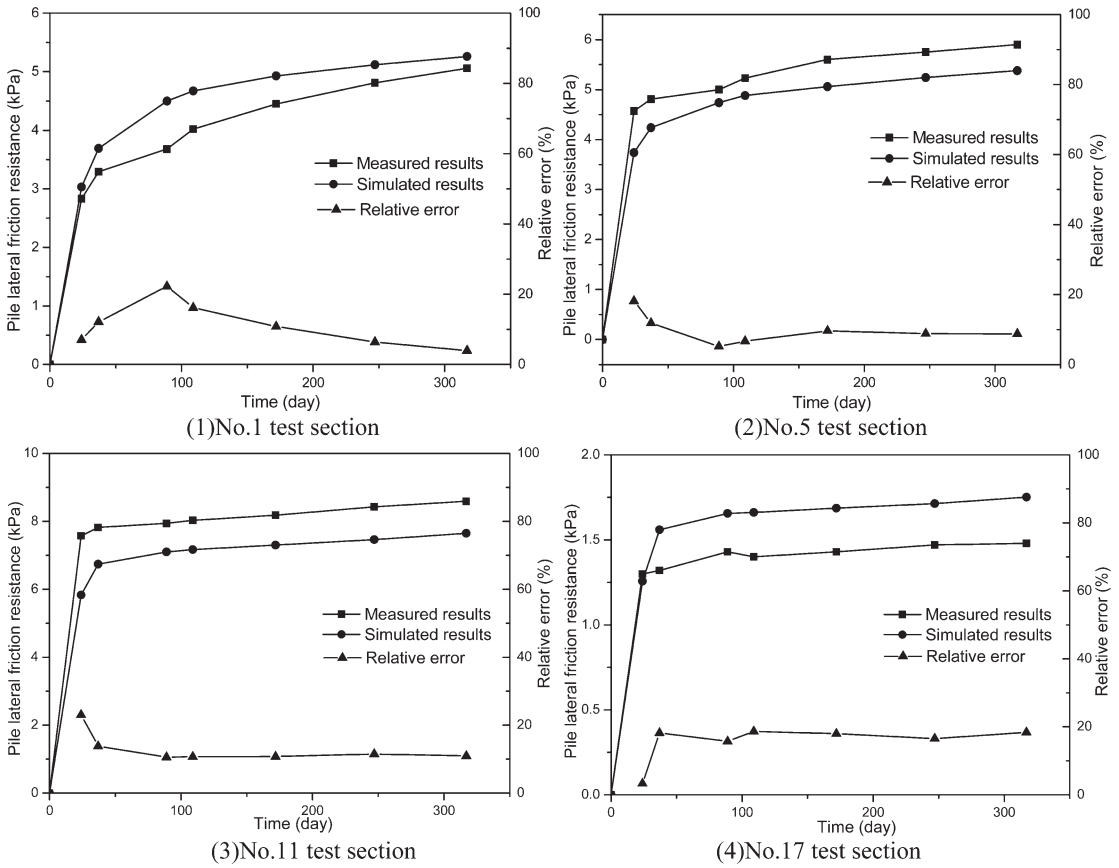

Figure 13: Comparison of the simulated pile lateral friction resistance and the measured results

sistent with the measured trend. The pile lateral frictional resistance rapidly changes with time during the early stages (0 d to 89 d) but tends to be flat in the latter stages. All of the relative error between the simulated pile lateral frictional resistance and the measured is less than 23%. In view of the high complexity of the actual pile-soil contact problems, the accuracy of the pile-soil interface constitutive model established in this paper is acceptable in simulating the pile-soil contact problems.

6. Conclusions

In this paper, the lateral friction resistance and pile-soil relative displacement of bridge piles in deep soft soils are monitored for 317 d, and the monitoring results reveal that the pile-soil interface of the pile foundation in soft soils is time dependent. However, given that the existing interface constitutive models do not consider the time effect, they cannot completely reflect the real pile-soil interface relationship in soft soils. For super-long pile foundations in deep soft soils, a pile-soil constitutive interface model must be established to accurately reflect the pile-soil interface relationship. Based on the Goodman model, the elasto-viscoplastic interface constitutive model of the pile-soil interface is proposed and developed into the FRIC subroutine in the ABAQUS software. The results of the field tests verified the efficiency of the proposed model. A favorable match is also observed between the simulated and measured pile lateral friction resistances and pile-soil relative displacements. The relative error between the simulated pile-soil relative displacement and the measured results is less than 15% in most cases, and all of the relative error between the simulated pile lateral frictional resistance and the measured results is less than 23%.

Acknowledgment

This work was supported by the Scientific Research Project of Shanghai Railway Bureau (No. 2013144) and the National Natural Science Foundation of China (No.11705083).

7. Nomenclature and abbreviations

$\underline{E}$	elastic modulus of the pile (Pa)
ε_i	average measured strain of section *i*
U	circumference of the pile section (m)
l_i	length between sections *i* and *i*+1 (m)
w_0	displacement of the pile top (m)
$\Delta\tau_1, \Delta\tau_2$	shear stress increments in two tangential directions of the interface (Pa)
$\Delta\gamma_1^e, \Delta\gamma_2^e$	elastic shear strain increments in two tangential directions of the interface
k_{s1}, k_{s2}	tangential stiffness coefficients in two tangential directions of the interface (Pa)
K, n, R_f	nonlinear indexes of the hyperbolic model proposed by **Clough and Duncan (1971)**
δ	interface friction angle of the interface (◦)
r_w	water unit weight (N/m^3)
P_a	atmospheric pressure (Pa)
σ_n	normal stress (Pa)
η	viscosity coefficient of the pile-soil interface (Pa.s)
F	yield function
F_0	reference value of the yield function
Φ	function that defines the viscoplastic strain rate
Q	plastic potential function
σ_{ij}	stress tensor of the interface (Pa)
Δt	time increment (s)
α, k	parameters of the Drucker–Prager yield criterion
J_2	second principal stresses invariant
I_1	major principal stress invariant
δ_{ij}	Kronecker delta
S_{ij}	deviatoric stress tensor

8. References

Abu-Farsakh, M., Souri, A., Voyiadjis, G & Rosti, F. (2017): Comparison of static lateral behavior of three pile group configurations using three-dimensional finite element modeling. Canadian Geotechnical Journal, 55, 2, 107-118. https://doi.org/10.1139/cgj-2017-0077.

An G. and Gao D. (2001): Research on elastic-visco-plastic constitution of interfaces. China Civil Engineering Journal, 34, 88~92. http://d.wanfangdata.com.cn/Periodical/tmgcxb200101017

Boulon, M. and Nova, R. (1990): Modelling of soil-structure interface behaviour a comparison between elastoplastic and rate type laws. Computers & Geotechnics, 9, 1, 21-46. https://doi.org/10.1016/0266-352x(90)90027-s.

Chen, L.Q., Yang, H.S & Lin H. (2011): Finite element analysis for slope stability and its influencing factors with pile reinforcement. Journal of Central South University, 23, 3, 175-184. http://en.cnki.com.cn/Article_en/CJFDTOTAL-ZNGD201102035.htm&ie=utf-8&sc_us=1559885113342337629.

Clough, G.W. and Duncan, J.M. (1971): Finite element analyses of retaining wall behavior. Journal of Soil Mechanics & Foundation Engineering, 97, 12,1657-1673. http://trid.trb.org/view/125555&ie=utf-8&sc_us=6907931132851557298.

Desai, C.S. and Zaman, M.M. (1984): Thin Layer Element for Interface and Joints. International Journal for Numerical & Analytical Methods in Geomechanics, 8, 1, 19~43. https://doi.org/10.1002/nag.1610080103.

Ghaboussi, J., Wilson, E.L. & Isenberg J. (1973): Finite Element for Rock Joints and Interface. Journal of the Soil Mechanics and Foundations Division, 834~848. https://doi.org/10.1016/0148-9062(74)91720-3.

Goodman, R.F., Tailor, R.L. & Brekke, T.L. (1968): A Model for the Mechanics of Jointed Rock. Journal of the Soil Me-

chanics and Foundations Division, 94, 637~660. http://trid.trb.org/view/126930&ie=utf-8&sc_us=18145494015754217554.

Gradiki, K., Mulabdi, M. & Minaek, K. (2017): Selected results of determining the friction interaction coefficient between crushed stone and polyester strip. Rudarsko Geolosko Naftni Zbornik, 32, 4, 37-43. http://hrcak.srce.hr/ojs/index.php/rgn/article/view/5064

Guo, W.D. (2000): Visco-elastic load transfer models for axially loaded piles. International Journal for Numerical & Analytical Methods in Geomechanics, 24, 2, 135-163. https://onlinelibrary.wiley.com/doi/10.1002/%28SICI%291096-9853%28200002%2924%3A2%3C135%3A%3AAID-NAG56%3E3.0.CO%3B2-8

Guo, W.D. (2000): Visco-elastic consolidation subsequent to pile installation. Computers & Geotechnics, 2000, 26, 2, 113-144. https://doi.org/10.1016/s0266-352x(99)00028-2.

Hussein, Y.A., He, Y.Y & Baydaa, H.,M. (2017): Dynamic response of bridge-ship collision considering pile-soil interaction. Civil Engineering Journal, 3, 10, 965-971. http://www.civilejournal.org/index.php/cej/article/view/437

Jun J. (2015): Prediction of the Settlement for the Vertically Loaded Pile Group Using 3D Finite Element Analyses. Marine Georesources & Geotechnology, 33, 3, 264-271. http://www.tandfonline.com/doi/full/10.1080/1064119X.2013.869285.

Li, Z., Wang, K., Lv, S. & Wu, W.,B. (2015): A new approach for time effect analysis in the settlement of single pile in nonlinear viscoelastic soil deposits. Journal of Zhejiang University Science, 16, 8, 630-643. http://orcid.org/0000-0002-9362-0326.

Liu, J., Gao, H. & Liu, H. (2012): Finite element analyses of negative skin friction on a single pile. Acta Geotechnica, 7, 3, 239-252. DOI: https://doi.org/10.1007/s11440-012-0163-x.

Mabsout, M.E. and Tassoulas, J.L. (2010): A finite element model for the simulation of pile driving. International Journal for Numerical Methods in Engineering, 37, 2, 257-278. http://onlinelibrary.wiley.com/doi/10.1002/nme.1620370206/pdf&ie=utf-8&sc_us=15870110415057493112.

Randolph, M.F. and Wroth, C.P. (1979): An analysis of the vertical deformation of pile groups. Geotechnique, 29, 4, 423~439. https://doi.org/10.1016/0148-9062(80)90432-5.

Sheng-yang, F., Li-min, W., He, Q. & Fu-liang, J. (2014): Elastic-viscoplastic constitutive modeling of soil-structure interface, 19, 2829-2838. http://www.ejge.com/2014/.

Swoboda, G. and Mertz, W. (1987): Rheological analysis of tunnel excavations by means of coupled finite element-(FEM)-boundary element(BEM) analysis. International Journal for Numerical and Analytical Methods in Geomechanics, 11, 2, 115~129. https://doi.org/10.1016/0148-9062(87)91176-4.

Yang, M. and Liu, S. (2015): Field tests and finite element modeling of a prestressed concrete pipe pile-composite foundation. Ksce Journal of Civil Engineering, 19, 7, 2067-2074. https://doi.org/10.1007/s12205-015-0549-z.

Yin, Z.Z., Zhu, H. & Xu, G.H. (1994): Numerical Simulation of the Deformation in the Interface between Soil and Structural Material. Chinese Journal of Geotechnical Engineering, 16, 3, 14-22. http://en.cnki.com.cn/article_en/cjfdtotal-ytgc403.001.htm&ie=utf-8&sc_us=10518829304658727389.

Zhao, M., Deng, Y., Liu, J., & He, S.H. (2013): Finite element analysis of displacements of double pile-column bridge piers at steep slope. Journal of Central South University, 20, 12, 3683-3688. https://doi.org/10.1007/s11771-013-1896-x.

Zhang Z.,Xin, G., & Xia, T. (2004): Test and research on unrock-socketed super-long pile in deep soft soil. China Civil Engineering Journal, 37, 4, 64~69. http://en.cnki.com.cn/Article_en/CJFDTOTAL-TMGC200404012.htm&ie=utf-8&sc_us=11318033163880418098.

Zou, X.J., Zhao, M.H. & Wu, B.L. (2006): Nonlinear finite element analysis of pile group under inclined loads in stratified subgrade. Journal of Central South University, 37, 4, 820-825. https://doi.org/10.1007/978-3-642-48013-3_13.

SAŽETAK

Vremenski utjecaj na međudjelovanje odlagališta i tla te njihov elastično-viskozno-plastični model

Međudjelovanje odlagališta (jalovine) i tla jedan je od najvažnijih problema kod izučavanja mehaničkih svojstava takvih odlagališta. Praćeno je bočno smicanje te otpor na dodiru mekoga tla i odloženoga materijala unutar njega tijekom vremena. Unutar testnoga odlagališta također su postavljeni betonski blokovi za mjerenje naprezanja. Rezultati su pokazali kako su bočna smicanja između odloženoga materijala i tla ovisna o vremenu. Ta zavisnost modelirana je elastično-viskozno-plastičnim modelom, čime je opisana ovisnost mehaničkih pojava o vremenu. Prikazani model deriviran je iz Goodmanova, te je rutinom (FRIC) opisan u programskome paketu (ABAQUS), koji je ujedno i najčešći program za analizu konačnih elemenata s ovakvom namjenom. Izračunani otpor na bočno smicanje te relativni pomaci u odlagalištu vrlo su slični onima izmjerenim na mjestu eksperimentalnoga testiranja. Također je potvrđena mogućnost predviđanja modelom promjena nastalih zbog naprezanja tijekom vremena.

Ključne riječi:
međudjelovanje odlagalište – tlo, vremenski utjecaj, elastično-viskozno-plastični model, otpor na bočno smicanje, relativni pomak između odlagališta i tla

Authors contribution

Hong-quan Li (Ph.D. candidate of civil Engineering in Central South University) carried out the field tests in this paper and wrote the paper. **Sheng-yang Feng** (Ph.D, Assistant professor of civil Engineering in the University of South China) established the pile-soil interface model and was responsible for writing the paper. **Li-min Wei** (Ph.D, Professor of civil Engineering in Central South University) provided the data and gave advice. **Zhi Chen** (Master student in the University of South China) helped to revise the paper.